

The Determination of the Crystal Structure of Pectolite, $Ca_2NaHSi_3O_9$

By **M. J. BUERGER**

With 15 figures

(Received August 20, 1956)

Zusammenfassung

Die Kristallstruktur des triklinen, zur Raumgruppe $P\bar{1}$ gehörenden Pektoliths wurde mit Hilfe von drei PATTERSON-Projektionen bestimmt.

Die PATTERSON-Projektion $P(xz)$ konnte gelöst werden nach Auffinden zweier konjugierter Spitzen im Diagramm. Diese legen zwei Paare von Spitzen, die durch Inversion einander zugeordnet sind, fest. Beide Paare wurden der Berechnung je einer Minimumfunktion zugrunde gelegt. Diese Funktionen vom Rang 2 ergaben kombiniert eine verstärkte Minimum-Funktion vom Rang 4, aus der die Struktur abgelesen werden konnte.

Die PATTERSON-Projektionen $P(xy)$ und $P(yz)$ und deren Lösungen durch die Minimum-Funktionen (sowie auch andere Fakten) zeigten, daß der Pektolith eine Unterstruktur besitzt, so daß es möglich war, die Unterstrukturtheorie anzuwenden. Dementsprechend wurden die partiellen PATTERSON-Projektionen gebildet. Die drei Projektionen des Pektoliths wurden dann durch FOURIER-Synthesen verfeinert.

Die Struktur des Pektoliths wurde bereits früher beschrieben.¹ Es ist eine vom Pyroxentyp verschiedene Kettenstruktur. Die *Na*-Atome haben eine ungewöhnliche Umgebung und zeigen eine beträchtliche anisotrope Wärmebewegung. Die *H*-Atome verbinden *O*-Atome von zwei verschiedenen Tetraedern.

Abstract

Pectolite is triclinic, space group $P\bar{1}$, with 15 nonhydrogen atoms in the asymmetric unit. Its crystal structure has been determined by solving the three PATTERSON projections by the use of image-seeking functions.

The PATTERSON projection $P(xz)$ was solved after finding two conjugate peaks on the map. These located two sets of inversion peaks upon each of which a scaled minimum function was based. These two functions of rank 2 were combined to give the more powerful minimum function of rank 4. This was such a good approximation to the electron density that the general nature of the structure could be deduced from it.

¹ M. J. BUERGER, The arrangement of atoms in crystals of the wollastonite group of metasilicates. Proc. Nat. Acad. Sci. **42** (1956) 113—116.

The PATTERSON projections $P(xy)$ and $P(yz)$, and their solution by minimum functions (as well as other evidence) suggested that pectolite has a substructure, so that it became possible to apply substructure theory^{2,3}. Accordingly, the partial PATTERSON projections $\partial P(xy)$ and $\partial P(yz)$ were computed and solved for the locations of the atoms of the complement structure. The three projections of pectolite were refined by successive FOURIER syntheses and by difference maps.

The structure of pectolite has already been described¹. It is based upon single silica chains differing from the pyroxene-type chains. The *Na* atoms have an unorthodox environment, and show considerable anisotropic thermal motion. The hydrogen atoms bond together oxygen atoms of two different tetrahedra.

Introduction

Pectolite was formerly regarded as monoclinic⁴. WARREN and BISCOE⁵, examining it by the oscillating-crystal method, noted that the spectra required triclinic, rather than monoclinic, symmetry. PEACOCK⁶ later confirmed the triclinic symmetry from a morphological study.

A brief note of the crystal structure of pectolite has already been published by the author¹ but the analysis was treated only in outline. A fuller account, describing the application of a new crystal-structure analysis method³ suitable to crystals like pectolite, is given here.

Material and cell data

Professor CLIFFORD FRONDEL of the Mineralogical Department of Harvard University kindly made available to the writer some of the pectolite from Paterson, New Jersey, studied by PEACOCK. The cell, and later the intensities, were studied by means of *c* axis and *a* axis precession photographs (dial axis *b**), and by means of *b* axis DE JONG-BOUMAN photographs. Table 1 shows the cell characteristics as determined in the study, compared with the older results of WARREN and BISCOE⁵ and of PEACOCK⁶. The new results are in good agreement with the older data.

² M. J. BUERGER, Some relations for crystals with substructures. Proc. Nat. Acad. Sci. **40** (1954) 125–128.

³ M. J. BUERGER, Partial FOURIER syntheses and their application to the solution of certain crystal structures. Proc. Nat. Acad. Sci. **42** (1956) 776–781.

⁴ EDWARD SALISBURY DANA and WILLIAM E. FORD, A Textbook of Mineralogy. (John Wiley & Sons, 1932) 567.

⁵ B. E. WARREN and J. BISCOE, The crystal structure of the monoclinic pyroxenes. Z. Kristallogr. **80** (1931) 391–401, especially 400–401.

⁶ M. A. PEACOCK, On pectolite. Z. Kristallogr. **90** (1935) 97–111.

Table 1. *Crystallographic data for pectolite*

Locality	Cell data		Axial ratios		
	WARREN and BISCOE ⁵	BUERGER	WARREN and BISCOE ⁵	PEACOCK ⁶	BUERGER
	Giellebekk, near Oslo, Norway	Paterson, N. J.	Giellebekk, near Oslo, Norway	Paterson and Union Hill, N. J.	Paterson, N. J.
<i>a</i>	7.91 Å	7.99 Å	1.115	1.1369	1.135
<i>b</i>	7.08	7.04	1	1	1
<i>c</i>	7.05	7.02	0.995	0.9993	0.997
α	90°	90° 31'	90°	90° 23 $\frac{1}{2}$ '	90° 31'
β	95° 10'	95° 11'	95° 10'	95° 14'	95° 11'
γ	103° 00'	102° 28'	103° 00'	102° 42 $\frac{1}{2}$ '	102° 28'
cell content space group	2Ca ₂ NaHSi ₃ O ₉ P $\bar{1}$ (or <i>P1</i>)				

Intensity determination

Intensities were measured by the M. I. T. modification of the DAWTON method⁷ from *a* axis and *c* axis precession photographs and *b* axis DE JONG-BOUMAN photographs. All measurements were made using *MoK α* radiation. The (100) and (001) cleavages of pectolite are extremely perfect, and there is no cleavage transverse to these. Consequently, any attempt to break a crystal results in producing indefinitely long splinters parallel to *b*. Partly for this reason and partly to establish the relation between morphology and structure, one of PEACOCK's original measured crystals was retained for the *a* axis and *c* axis precession photographs. Since this was a comparatively large crystal for intensity determination, it is known that the *hk0* and *0kl* intensities are subject to errors due to absorption. A smaller cleavage splinter was used for the DE JONG-BOUMAN photographs, so that the *h0l* intensities are more reliable.

Some interesting intensity relations. The *c* axis precession photographs revealed some interesting relations among the *hk0* intensities. In the first place it was apparent that the rows of the reciprocal lattice having *k* even were related by a symmetry plane perpendicular to the *b* axis, as first noted by WARREN and BISCOE⁵. But it was further

⁷ RALPH H. V. M. DAWTON, The integration of large numbers of X-ray crystal reflections. Proc. Physic. Soc. **50** (1938) 919–925.

noted that the strong reflections near the origin formed a diamond-shaped lattice, as shown in Fig. 1. The relation of this supercell in reciprocal space to the true reciprocal cell is

$$\begin{aligned} A^* &= a^* + 2b^* \\ B^* &= -2a^* - 2b^* \end{aligned}$$

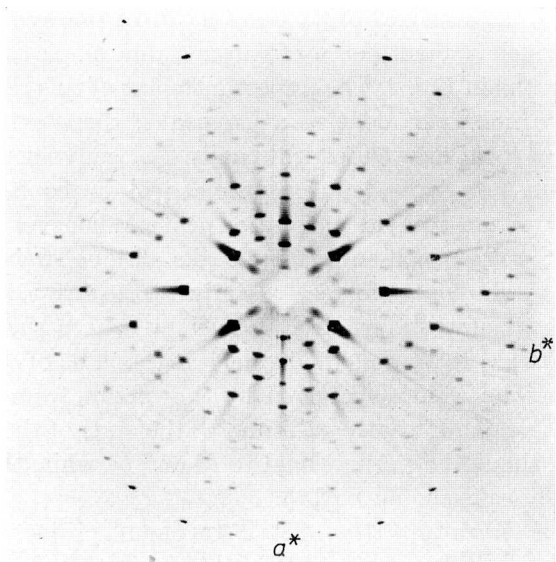


Fig. 1. Precession photograph of pectolite (precessing axis is c)

This suggests that the unit cell in direct space contains a substructure². The period of the substructure in the b direction is $b/2 = 3.52 \text{ \AA}$. This is what would be expected if CaO_6 octahedra shared edges to form chains parallel to b . The period of the substructure at right angles to b is such that it does not correspond well with a sheet of CaO_6 octahedra parallel to the plane (001), for in this case the substructure would be based upon a nearly perfect hexagonal sublattice.

As a result of these intensity observations, it is obvious that pectolite can be regarded as having a substructure with period $b/2$. The hypothesis was also tentatively entertained that the structure contains CaO_6 octahedra sharing edges and having a subperiod $b/2$.

Structure determination

General outline. The structure was determined entirely by solving PATTERSON projections by means of minimum functions. The projection $P(xz)$ was solved by straightforward methods. On the other hand,

a new partial PATTERSON function was devised to solve the xy and yz projections.

Conjugate peaks. A PATTERSON synthesis is most easily solved if one can find a single peak⁸. If the crystal has any kind of reflection symmetry, such a peak can often be located with the aid of reflection satellites⁹. The symmetry of pectolite is without reflection planes, and the symmetry of its several projections is $p2$. In this symmetry, there is a relation which is sometimes useful in revealing single rotation peaks. This is illustrated in Fig. 2. The important point of this relation is that for every two non-equivalent rotation peaks, there exists two non-equivalent *but equal* unsymmetrical peaks. For convenience, let these two equal but non-equivalent unsymmetrical peaks be called *conjugate* to the two non-equivalent rotation peaks. Whenever a PATTERSON projection shows two non-equivalent peaks of equal weight, they can be regarded as candidates for peaks conjugate to two sets of rotation peaks. The geometry shown in Fig. 2 shows where the two sets of rotation peaks are to be sought, namely at the ends of diagonals of a parallelogram whose sides are given by the vectors from the origin to the conjugate peaks. If peaks are found at the ends of these diagonals, their weights should be proportional to a^2 and b^2 , while the weights of the conjugate peaks should be $2ab$.

Solution of the xz projection. The PATTERSON projection $P(xz)$ for pectolite is shown in Fig. 3. A study of this projection shows two peaks which are non-equivalent yet equal. If these are taken as conjugate peaks of weight $2ab$, then the candidate rotation peaks are readily found and have weights which are acceptable as a^2 and b^2 . With two rotation peaks established, it becomes possible to form minimum functions $M_2(xz)$ for each of them independently. If these are to be combined to form the more powerful minimum function $M_4(xz)$, each must be properly weighted⁸; specifically, if the peak of weights a^2 is regarded, as standard then the ${}^aM_2(xz)$, formed by using a^2 as image point, is weighted as $a/a = 1$, while the ${}^bM_2(xz)$, formed by using b^2 as image point, is to be weighted by a/b .

The properly weighted minimum function ${}^aM_2(xz)$ and ${}^bM_2(xz)$ found from $P(xz)$ of pectolite are shown in the upper part of Fig. 4.

⁸ M. J. BUERGER, A new approach to crystal-structure analysis. *Acta Crystallogr.* **4** (1951) 531–544.

⁹ MARTIN J. BUERGER, Proyecciones de PATTERSON de cristales simétricos. *Anales de la Real Sociedad Española de Física y Química* **50** (A) 221–254, especially 231–237.

Their combination to form the more powerful ${}^{ab}M_4(xz)$ is shown in the lower part of Fig. 4. This must be a fair approximation to the electron density, $\varrho(xz)$, of pectolite. If it can be interpreted, it can be readily refined.

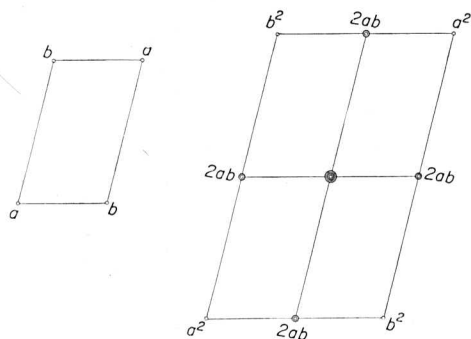


Fig. 2. Relation between two rotation peaks and their conjugate peaks

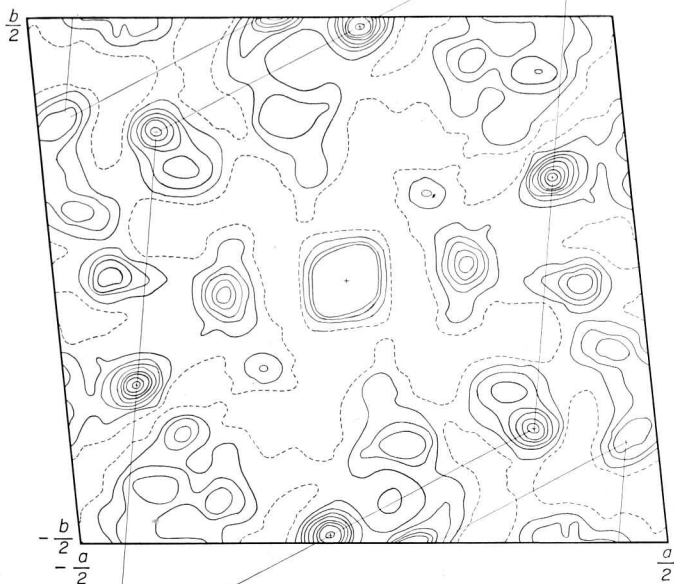


Fig. 3. The PATTERSON projection $P(xz)$ for pectolite; origin at center

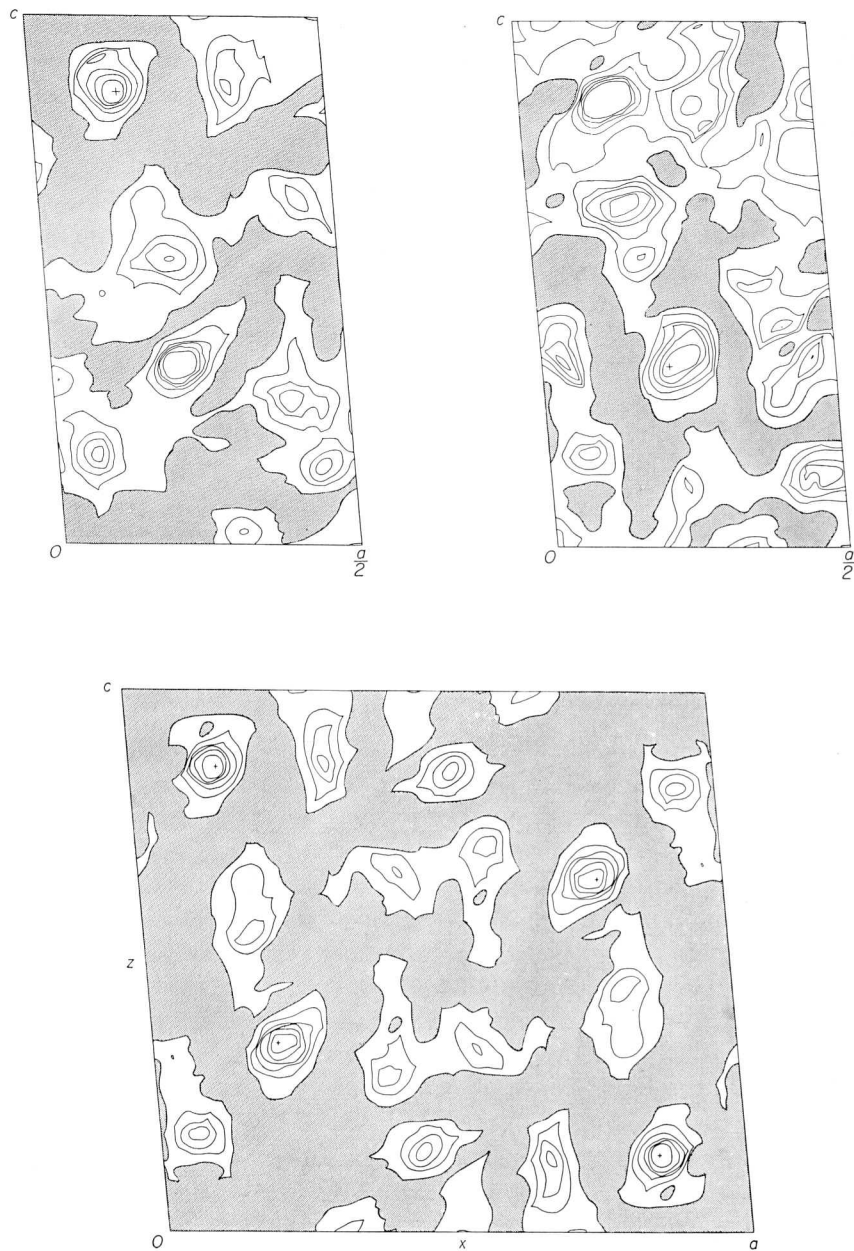


Fig. 4. The upper two diagrams show the properly weighted minimum functions ${}^aM_2(xz)$ and ${}^bM_2(xz)$ for pectolite, derived from Fig. 3. The lower diagram shows the combination of these to form the more powerful minimum function ${}^{ab}M_4(xz)$.

Upper diagrams are half cells; lower diagram is a full cell

The possibility, noted in an earlier section, that CaO_6 octahedra share edges parallel to b requires two Ca atoms to be superposed in this projection. This should show up as a heavy peak in the minimum function, and it should be surrounded by oxygen atoms in such a way as to be consistent with octahedral coordination about the Ca atoms. With this start, the upper left strong peak in $M_4(xz)$ was identified as $Ca_1 + Ca_2$. The lower left heavy peak was then identified as $Si_1 + Si_2 + O_9$, surrounded by the triangular base of the tetrahedral oxygen environment. The remaining unaccounted-for peaks were assigned, in order of decreasing weight, to Si_3 and Na .

With this assignment of atoms to peaks, the general nature of the structure projected on xz was apparent. It was refined in a preliminary way by repeated FOURIER syntheses. The final projection, $\rho(xz)$, is shown in Fig. 5. A comparison of $\rho(xz)$ in Fig. 5 with $M_4(xz)$ at the bottom of Fig. 4 shows how well the latter approximated the true electron density.

Solution of the xy projection. The PATTERSON projection $P(xy)$ for pectolite is shown in Fig. 6. The pattern of this projection closely resembles that which might be expected of a crystal with period $b/2$ rather than b . This is an aspect of the strong substructure feature

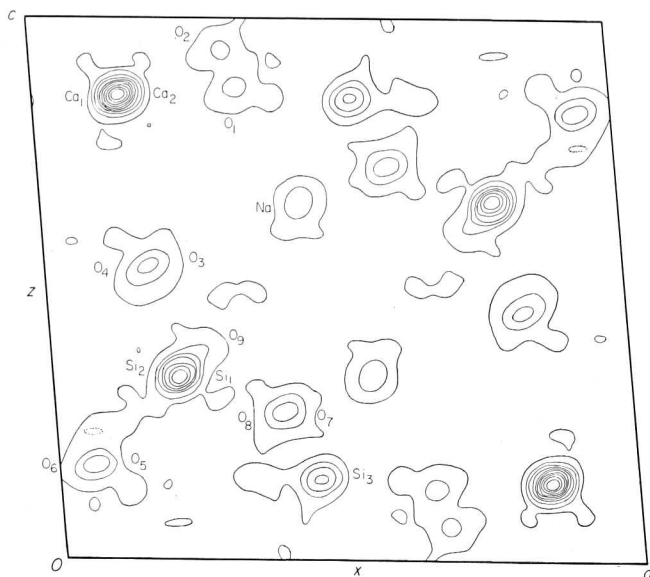


Fig. 5. The electron-density projection $\rho(xz)$ for pectolite. Compare with the lower part of Fig. 4

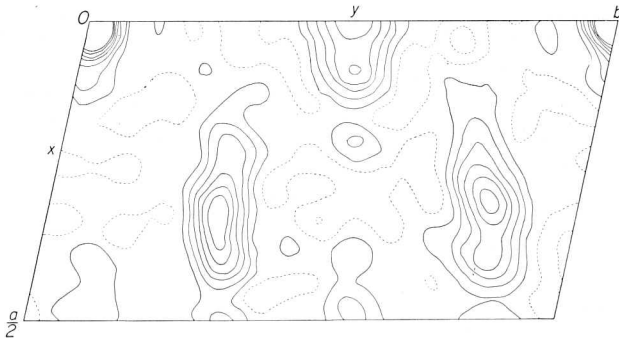


Fig. 6. The PATTERSON projection $P(xy)$ for pectolite

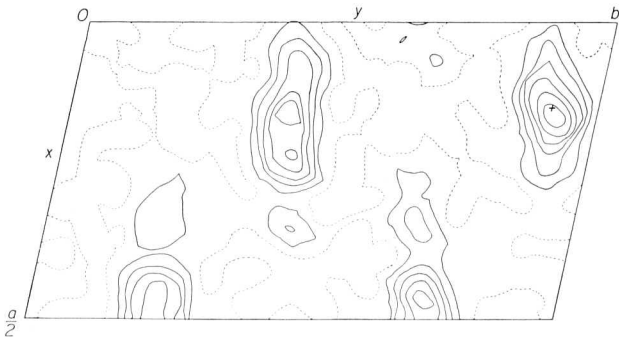


Fig. 7. The minimum function $M_2(xy)$ for pectolite

already mentioned. The solution of the xz projection, given in the last section, locates the x coordinates of the Ca_1 and Ca_2 atoms. The assumption that the sharing of edges of CaO_6 octahedra to form chains parallel to b accounts for the $b/2$ pseudo period and fixes the y coordinates of the Ca_1 and Ca_2 atoms.

The xy locations of the Ca_1 and Ca_2 atoms, established in this manner, permits identification of the two major peaks of the PATTERSON projection $P(xy)$ as rotation peaks for these atoms. Using one of these as the end of a line image, the minimum function $M_2(xy)$ can be formed, and this is shown in Fig. 7. This necessarily shows the pseudo-period $b/2$ since the image point of both Ca_1 and Ca_2 rotation peaks is the same. Such a minimum function is difficult to interpret in respect to atoms not involved in the subperiod.

To overcome this disadvantage, the partial PATTERSON synthesis³ was devised. In this case, since the substructure has period $b/2$, the substructure contributes only to reciprocal lattice points with period

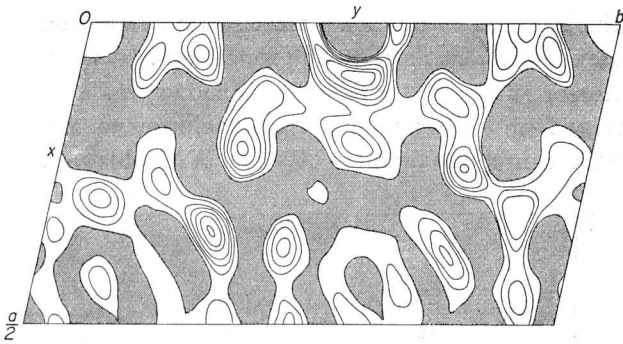


Fig. 8. The partial PATTERSON projection $\partial P(xy)$ for pectolite, using only $F^2(hk0)$ for k odd

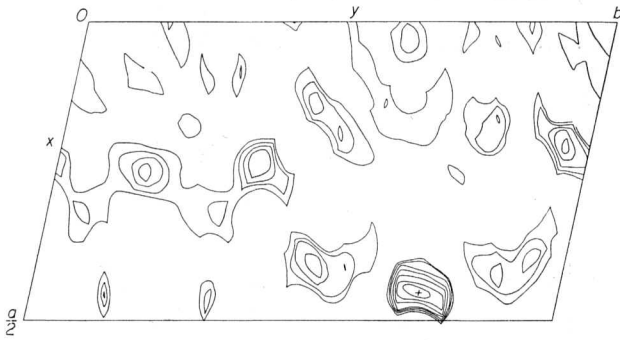


Fig. 9. The minimum function $\partial M_2(xy)$ derived from Fig. 8

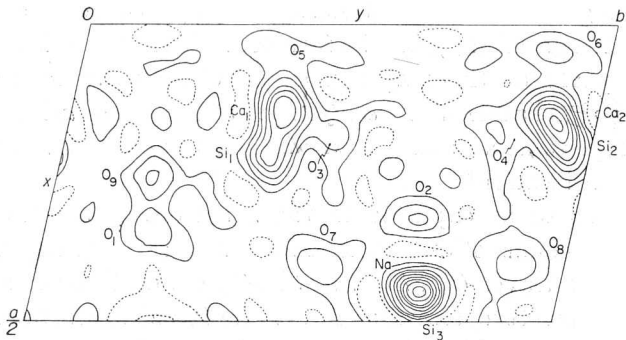


Fig. 10. The electron density $\rho(xy)$ for pectolite. Compare the substructure-atom locations with Fig. 7, and compare the complement-structure-atom locations with Fig. 9

2b*. A partial PATTERSON synthesis which eliminates the substructure can be constructed by using only the reflection $hk0$ with k odd. This partial Patterson, $\partial P(xy)$, for pectolite is shown in Fig. 8. It contains a strong peak which bears a rotation-peak relation to the third strong peak in the full minimum function $M_2(xy)$. With this peak as one end

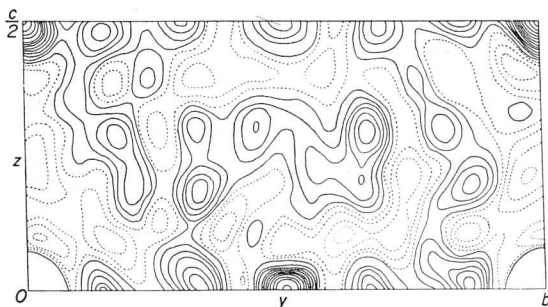


Fig. 11. The PATTERSON projection $P(yz)$ for pectolite

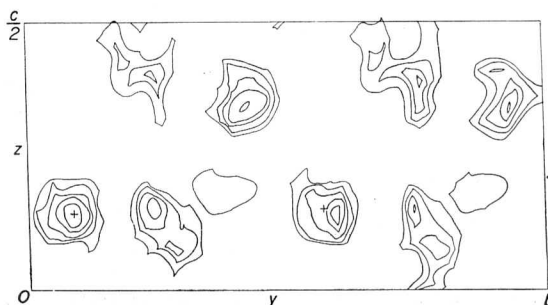


Fig. 12. The minimum function $M_2(yz)$ for pectolite, derived from Fig. 11

of a line image, the minimum function $\partial M(xy)$, corresponding to the partial Patterson $\partial P(xy)$, can be formed. It is shown in Fig. 9. All of the strong peaks on this map correspond either to atoms not in the *substructure* (but rather in the *complement structure*), or, where the area looks incomplete as an atom, to deviations of the substructure atom from an ideal location³.

The atoms to be expected in the substructure are those which pertain to the chains of CaO_6 octahedra. These are $Ca_1, Ca_2, O_1, O_2, O_3, O_4, O_5, O_6$. This leaves $Ca_3, Si_1, Si_2, Si_3, O_7, O_8, O_9$ to be found in the complement structure, and therefore to be found in the partial minimum function map $\partial M_2(xy)$. The x coordinates of these atoms, known from $\rho(xz)$, help locate them in $\partial M_2(xy)$. It turns out that Ca_3 and Si_3 are superposed in $\partial M_2(xy)$, and that O_3 and O_4 show a considerable

deviation from ideal substructure locations. After refinement of the entire structure by successive FOURIER synthesis, the electron density is as shown in Fig. 10. This should be compared with $\partial M_2(xy)$ to understand how well solution of the partial Patterson provided the locations of the atoms of the complement structure.

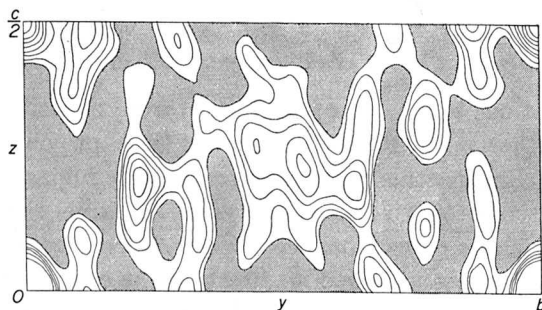


Fig. 13. The partial PATTERSON projection $\partial P(yz)$ for pectolite, using only $F^2(0kl)$ for k odd

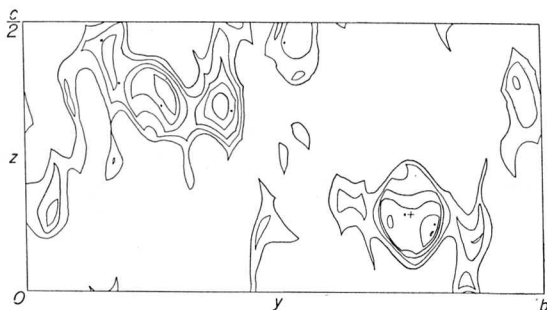


Fig. 14. The minimum function $\partial M_2(yz)$ derived from Fig. 13

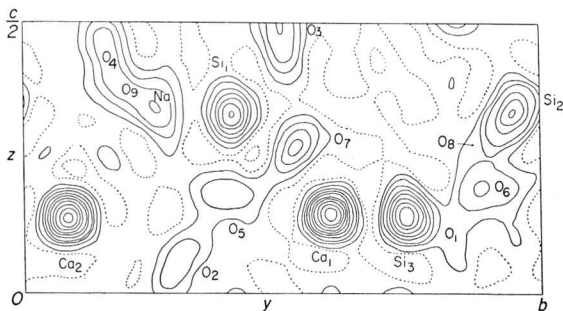


Fig. 15. The electron density $\rho(yz)$ for pectolite. Compare the substructure-atom locations with Fig. 12, and compare the complement-structure-atom locations with Fig. 14

Solution of the yz projection. With the xz and xy projections established, the yz projection is fixed. The projection can also be determined directly as was the xy projection. Figs. 11, 12, 13, 14 and 15 show $P(yz)$, $M_2(yz)$, $\partial P(yz)$, $\partial M_2(yz)$, and $\rho(yz)$ respectively. Again, it is interesting to compare Figs. 14 and 15 to see how faithfully $\partial M_2(yz)$ has provided the complement structure of $\rho(yz)$.

Refinement

The projections $\rho(xy)$, $\rho(yz)$, and $\rho(xz)$ were refined somewhat by difference synthesis. The final R factors for these projections are 16%, 21%, and 25%, respectively. The comparatively high values of these factors are attributed to using a crystal so large that absorption effects (for which no corrections were made) were severe. The electron density projections, especially Fig. 10, show the effects of this absorption error in the overemphasis of the F 's of high $\sin \theta$ values.

The difference maps revealed that the Na atoms undergo considerable anisotropic temperature motion.

The structure

The final parameters of pectolite are shown in Table 2. The interatomic distances for these parameters are given in Table 3. The general nature of the structure has already been briefly discussed¹.

Table 2. *Coordinates for atoms in pectolite*

	x	y	z
Ca_1	0.144	0.405	0.855
Ca_2	.154	.916	.861
Na	.448	.735	.657
Si_1	.222	.403	.336
Si_2	.209	.953	.345
Si_3	.454	.736	.145
O_1	.349	.207	.877
O_2	.327	.706	.948
O_3	.182	.492	.541
O_4	.167	.844	.534
O_5	.074	.395	.172
O_6	.053	.893	.184
O_7	.396	.532	.272
O_8	.397	.911	.278
O_9	.254	.184	.390

Table 3. *Interatomic distances in pectolite* Si_1 tetrahedron

	O_3	O_5	O_7	O_9
Si_1 xyz	1.60	1.64	1.70	1.63
O_3 xyz		2.80	2.57	2.49
O_5 xyz			2.81	2.58
O_7 xyz				2.81
O_9 xyz				

 Si_2 tetrahedron

	O_4	O_6	O_8	O_9
Si_2 x y z	1.57	1.72	1.61	1.69
O_4 x y z		2.64	2.62	2.68
O_6 x y z			2.82	2.95
O_8 x y z				2.39
O_9 x $1+y$ z				

 Si_3 tetrahedron

	O_1	O_2	O_7	O_8
Si_3 x y z	1.62	1.72	1.75	1.62
O_1 $1-x$ $1-y$ $1-z$		2.91	2.92	2.47
O_2 x y $z-1$			2.64	2.77
O_7 x y z				2.67
O_8 x y z				

Between tetrahedra

O_3 xyz	O_4 xyz	2.48
O_5 xyz	O_6 xyz	3.51

 Ca_1 octahedron

	O_1	O_2	O_5'	O_6'	O_3	O_5
Ca_1 x y z	2.18	2.63	2.27	2.61	2.31	2.30
O_1 x y z		3.56	4.45	3.30	3.38	3.33
O_2 x x z			3.37	5.22	3.41	3.35
O_5' $-x$ $1-y$ $1-z$				3.51	3.00	3.07
O_6' $-x$ $1-y$ $1-z$					3.80	3.35
O_3 x y z						4.57
O_5 x y $z+1$						

Ca₂ octahedron

				<i>O</i> ₂	<i>O</i> ₁	<i>O</i> _{6''}	<i>O</i> _{5'}	<i>O</i> ₄	<i>O</i> ₆
<i>Ca</i> ₂	<i>x</i>	<i>y</i>	<i>z</i>	2.13	2.55	2.18	2.83	2.35	2.42
<i>O</i> ₂	<i>x</i>	<i>y</i>	<i>z</i>		3.56	4.29	3.36	3.32	3.07
<i>O</i> ₁	<i>x</i>	1 + <i>y</i>	<i>z</i>			3.30	3.56	3.78	3.87
<i>O</i> _{6''}	- <i>x</i>	2 - <i>y</i>	1 - <i>z</i>				3.54	3.26	3.11
<i>O</i> _{5'}	- <i>x</i>	1 - <i>y</i>	1 - <i>z</i>					3.27	3.35
<i>O</i> ₄	<i>x</i>	<i>y</i>	<i>z</i>						4.67
<i>O</i> ₆	<i>x</i>	<i>y</i>	<i>z</i> + 1						

Na polyhedron

				<i>O</i> ₃	<i>O</i> ₄	<i>O</i> ₂	<i>O</i> ₃	<i>O</i> _{4'}	<i>O</i> ₁	<i>O</i> ₇	<i>O</i> ₈
<i>Na</i>	<i>x</i>	<i>y</i>	<i>z</i>	2.83	2.53	2.27	3.65	4.46	4.11	3.08	2.96
<i>O</i> ₃	<i>x</i>	<i>y</i>	<i>z</i>		2.48	3.42			3.38	2.57	
<i>O</i> ₄	<i>x</i>	<i>y</i>	<i>z</i>			3.32					2.61
<i>O</i> ₂	<i>x</i>	<i>y</i>	<i>z</i>							2.64	2.78
<i>O</i> ₃	1 - <i>x</i>	1 - <i>y</i>	1 - <i>z</i>								
<i>O</i> _{4'}	1 - <i>x</i>	2 - <i>y</i>	1 - <i>z</i>								
<i>O</i> ₁	1 - <i>x</i>	1 - <i>y</i>	1 - <i>z</i>							2.93	2.46
<i>O</i> ₇	<i>x</i>	<i>y</i>	<i>z</i>								2.67
<i>O</i> ₈	<i>x</i>	<i>y</i>	<i>z</i>								

Crystallographic Laboratory Massachusetts Institute of Technology
Cambridge, Massachusetts, U. S. A.